ELSEVIER

Journal of Organometallic Chemistry 562 (1998) 97–104

Journal of Organometallic Chemistry

Substitutional photochemistry of sandwich and half-sandwich complexes of ruthenium(II)[1]

Richard J. Lavallee [2], Charles Kutal *

Department of Chemistry, University of Georgia, Athens, Georgia 30602, USA

Received 3 December 1997

Abstract

Ruthenium(II) sandwich complexes of the type $Ru(\eta^6\text{-arene})_2^{2+}$ (arene is benzene or 1,3,5-trimethylbenzene) undergo photosubstitution of one arene ring by solvent (S) to yield $Ru(\eta^6\text{-arene})(S)_3^{2+}$. Reaction occurs from the lowest ligand field triplet state of the complex with a quantum efficiency that decreases with increasing methylation of the arene. Half-sandwich complexes of general formula $Ru(\eta^6\text{-arene})(L)_3^{2+}$ (L is CH_3CN or NH_3) undergo competitive photosubstitution of arene and L by solvent. The relative importance of these pathways depends upon a number of factors, including excitation wavelength, solvent, and the nature of L. Mechanisms for these photoreactions are discussed and comparisons to earlier studies are presented.

Keywords: Photosubstitution; Ruthenium(II) complexes; Arene complexes

1. Introduction

Karlen et al. [1] and the present authors [2] recently investigated the solution photochemistry of metal-sandwich complexes of general formula $Ru(\eta^6\text{-arene})_2^{2+}$. Both groups observed that irradiation into the ligand field absorption bands of these low-spin, d^6 complexes results in the substitution of one arene ring by three solvent molecules (Eq. 1; S is solvent). The key photochemical step appears to be the formation of an intermediate, **I**, containing an η^4-bonded arene ring and a coordinated solvent molecule. Subsequent thermal reactions of **I** with free solvent completes the deligation of the ring-slipped arene to yield the half-sandwich photoproduct, $Ru(\eta^6\text{-arene})(S)_3^{2+}$.

$$Ru(\eta^6\text{-arene})_2^{2+} \xrightarrow[CH_3CN]{h\nu} Ru(\eta^6\text{-arene})(S)_3^{2+} + \text{arene} \quad (1)$$

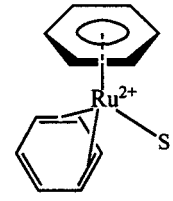

I

* Corresponding author. Fax: +1 706 5429454; e-mail: ckutal@sunchem.chem.uga.edu

[1] Dedicated to Professor R. Bruce King on the occasion of his 60th birthday.

[2] Present address: Department of Chemistry, St. Cloud State University, 720 Fourth Avenue South, St. Cloud, Minnesota 56301, USA.

0022-328X/98/$19.00
PII S0022-328X(98)00397-0

Prolonged irradiation of the system results in the secondary photolysis of the half-sandwich complex. A detailed examination [2] of this process for Ru(η^6-mes)$(CH_3CN)_3^{2+}$ (mes is 1,3,5-trimethylbenzene or mesitylene) in acetonitrile revealed that ligand-field excitation causes the release of the mesitylene ligand to yield the fully solvated metal ion (Eq. 2a). Precedent for this behavior is provided by the work of Weber and Ford [3], who reported that several Ru(η^6-arene)$(H_2O)_n(NH_3)_{3-n}^{2+}$ complexes follow a similar pathway in aqueous solution. Quite interesting, however, is our observation that Ru(η^6-mes)$(CH_3CN)_3^{2+}$ also undergoes efficient photochemical exchange of coordinated and free CH_3CN (Eq. 2b). In contrast, negligible photolabilization of NH_3 was observed for Ru(η^6-bz)$(NH_3)_3^{2+}$ and Ru(η^6-bz)$(H_2O)(NH_3)_2^{2+}$ (bz is benzene) [3]. Several factors could contribute to this striking disparity in the quantum efficiencies of monodentate ligand substitution measured in the two studies: these include the use of different (i) arenes (benzene vs. mesitylene), (ii) monodentate ligands (σ-bonding NH_3 vs. σ-bonding and π-backbonding CH_3CN), and (iii) solvents (H_2O vs. CH_3CN).

$$\text{Ru}(\eta^6\text{-mes})(\text{CH}_3\text{CN})_3^{2+} \xrightarrow{h\nu} \begin{cases} \xrightarrow{\text{CH}_3\text{CN}} \text{Ru}(\text{CH}_3\text{CN})_6^{2+} + \text{mes} & (2a) \\ \xrightarrow{\text{CD}_3\text{CN}} \text{Ru}(\eta^6\text{-mes})(\text{CH}_3\text{CN})_{3-n}(\text{CD}_3\text{CN})_n^{2+} & (2b) \end{cases}$$

We have now extended our investigation of the photosubstitutional chemistry of half-sandwich complexes of Ru(II) to include Ru(η^6-bz)$(CH_3CN)_3^{2+}$, Ru(η^6-bz)$(NH_3)_3^{2+}$, and Ru(η^6-mes)$(NH_3)_3^{2+}$. Irradiation of these complexes in CH_3CN results in competitive replacement of the arene and monodentate ligands by solvent (analogous to Eq. 2a, b). Reported here are quantum yield data that allow us to assess the relative contributions of these pathways in different complexes and, in particular, to determine the importance of factors (i)–(iii) noted above. Results of a complementary photochemical investigation of Ru(η^6-bz)$_2^{2+}$ and Ru(η^6-mes)$_2^{2+}$ also are described. The information presented should prove useful to those interested in applications that utilize these Ru(II) complexes as photocatalysts [4] or photoinitiators [5].

2. Experimental

2.1. Materials and syntheses

All chemicals were at least reagent grade quality and used as received from the supplier (Aldrich Chemical, unless noted otherwise). Solvents were HPLC grade and used without further purification. Acetophenone was purified by distilling twice under a nitrogen atmosphere.

Analytically pure samples of [Ru(η^6-bz)$_2$]$(PF_6)_2$, [Ru(η^6-mes)$_2$]$(PF_6)_2$, and [Ru(η^6-arene)$(CH_3CN)_3$]$(PF_6)_2$ were synthesized by previously described procedures [2,6,7], while the [Ru(η^6-arene)$(NH_3)_3$]$(PF_6)_2$ complexes were prepared from the corresponding [Ru(η^6-arene)Cl_2]$_2$ dimers using the method of Weber and Ford [3]. Isotopically-labeled [Ru(η^6-bz)$(^{15}NH_3)_3$]$(PF_6)_2$ was synthesized in an identical manner, except that the procedures were scaled down by a factor of four, and the source of aqueous ammonia was 14 N $^{15}NH_4OH$ (Isotec).

2.2. Instrumentation

Electronic absorption spectra were recorded on a Varian DMS 300 spectrophotometer. Luminescence measurements were performed on a Perkin Elmer MPF-44B spectrofluorimeter. ^{1}H-NMR spectra were taken on a Bruker AC-250 spectrometer operating at 250.134 MHz. Chemical shifts were referenced to internal tetramethylsilane (TMS) by assigning the solvent peak a value of 1.95 ppm. Prior to quantitative measurements, appropriate relaxation delays (typically 20–30 s) between successive scans were determined by evaluating the spin-lattice (T_1) relaxation times for signals of interest.

2.3. Quantum yield measurements

Quantum yields were determined via the photolysis of magnetically-stirred samples contained in 1.0 cm pathlength quartz cells maintained at 21.0 ± 0.5°C. Photolyses at 313 and 365 nm were performed using an Illumination Industries Model LH351P high-pressure mercury arc lamp situated 34 cm from the sample; the desired wavelengths were isolated by use of a quartz-faced water filter and an appropriate bandpass interference filter (width at half-height of 12 nm at 313 nm and either 25 or 31 nm at 365 nm). For experiments at 254 nm, the direct output of an Ultra-violet Pen-Ray low-pressure mercury lamp situated 2 cm from the sample was used. Typical concentrations of metal complexes were $4–6 \times 10^{-3}$ M. Corrections for inner filter effects

and incomplete light absorption were applied when the spectral characteristics of the photoproducts were known. Light intensities at all wavelengths were determined by potassium ferrioxalate actinometry [8].

The extent of photolysis of $Ru(\eta^6\text{-bz})_2^{2+}$ in CH_3CN was quantified spectrophotometrically by measuring the increase in solution absorbance at 400 nm, a wavelength at which $Ru(\eta^6\text{-bz})_2^{2+}$ and $Ru(\eta^6\text{-bz})(CH_3CN)_3^{2+}$ have extinction coefficients of 3.2 and 344 $M^{-1}\,cm^{-1}$, respectively. Typically, 5–10% of the starting material was reacted for quantum yield measurements.

Photosubstitution processes of $Ru(\eta^6\text{-bz})(CH_3CN)_3^{2+}$ in CD_3CN solution were monitored by ^{1}H-NMR spectroscopy. The extent of arene deligation was determined from the ratio of the area of the ring proton signal of free arene to the total ring proton area of the sample. Photochemical solvent exchange was quantified by measuring the decrease of the coordinated solvent signal area, corrected for the calculated thermal exchange using the previously determined pseudo first-order rate constant.

^{1}H-NMR spectroscopy also was employed to follow the photosubstitution reactions of $Ru(\eta^6\text{-arene})(NH_3)_3^{2+}$ in CD_3CN. For these complexes, the areas arising from the ring proton signals of free arene and $Ru(\eta^6\text{-arene})(NH_3)_2(CD_3CN)^{2+}$ provided measures of arene and NH_3 loss, respectively. Since corrections for competitive absorption of light by the multiple photoproducts could not be calculated explicitly, the quantum yields for each process were determined at different extents of reaction and then extrapolated to zero percent reaction. Photochemical ammine loss from $Ru(\eta^6\text{-bz})(^{15}NH_3)_3^{2+}$ was confirmed by monitoring the appearance of the signals due to the ammine ligands of $Ru(\eta^6\text{-bz})(^{15}NH_3)_2(CH_3CN)^{2+}$.

2.4. Sensitization experiments

Sensitization studies were performed in CH_3CN solutions containing 5.04×10^{-2} M acetophenone and concentrations of $Ru(\eta^6\text{-mes})_2^{2+}$ ranging from 3.92×10^{-4} to 3.92×10^{-3} M. Total sample absorbance was > 2.5 at the 313 nm excitation wavelength, and most of the incident light (70–96%) was absorbed by the sensitizer. Each sample was thoroughly degassed via three freeze-pump-thaw cycles prior to irradiation, and the extent of reaction of $Ru(\eta^6\text{-mes})_2^{2+}$ was quantified spectrophotometrically by monitoring the increase in absorbance at 400 nm. Corrections for the contribution from direct photolysis of the complex were applied as necessary, employing the previously determined quantum yield at 313 nm. Quantum yields for arene loss, Φ_{arene}, were determined for samples containing various $Ru(\eta^6\text{-mes})_2^{2+}$ concentrations. The limiting quantum yield at infinite complex concentration was determined from the y-intercept of the double-reciprocal plot of Φ_{arene} versus $Ru(\eta^6\text{-mes})_2^{2+}$ concentration.

3. Results and discussion

3.1. Spectroscopy and photochemistry of $Ru(\eta^6\text{-arene})_2^{2+}$ complexes

The electronic absorption spectrum of $Ru(\eta^6\text{-bz})_2^{2+}$ in room-temperature CH_3CN is shown in Fig. 1. By reference to the reported molecular orbital diagram for the complex [1], we assign the low-intensity band at 331 nm as the first spin-allowed ligand field transition, $^1A_{1g} \rightarrow a^1E_{1g}$ (D_{6h} symmetry). Shoulders appearing at ca. 284 and ca. 262 nm most likely correspond to the $^1A_{1g} \rightarrow (^1B_{1g}, {}^1B_{2g})$ and $^1A_{1g} \rightarrow b^1E_{1g}$ ligand field transitions, respectively, where we have assumed that the splitting of the $^1B_{1g}$ and $^1B_{2g}$ levels is too small to detect [9]. No feature attributable to the first spin-forbidden ligand field transition, $^1A_{1g} \rightarrow {}^3E_{1g}$, is detected out to 600 nm. A similar absence was noted in the case of $Ru(\eta^6\text{-mes})_2^{2+}$ [2]. Moreover, neither complex phosphoresces in argon-bubbled CH_3CN at room temperature. This lack of spectroscopic information makes it difficult to locate the lowest ligand field triplet state in these complexes. For use in the later discussion of sensitization, we estimate that the energy of this state is < 70 kcal by analogy to the triplet state energy of the related d^6 sandwich complex, ruthenocene [10]. The absorption spectrum of $Ru(\eta^6\text{-bz})_2^{2+}$ also contains a shoulder at 214 nm that lies on the tail of an intense absorption extending below 200 nm. The corresponding features in the spectrum of $Ru(\eta^6\text{-mes})_2^{2+}$ appear at lower energies, suggesting that the transitions involved contain

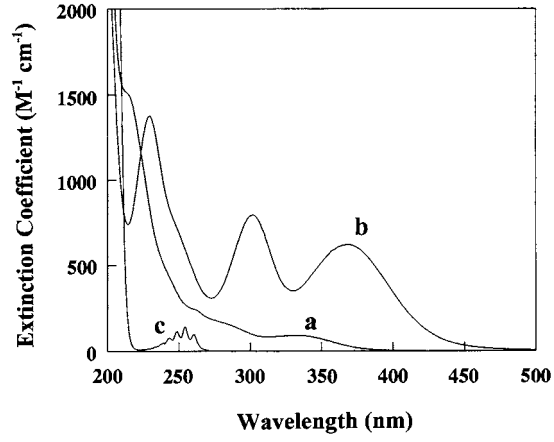

Fig. 1. Room-temperature electronic absorption spectrum of (a) $Ru(\eta^6\text{-bz})_2^{2+}$, (b) $Ru(\eta^6\text{-bz})(CH_3CN)_3^{2+}$, and (c) benzene in CH_3CN.

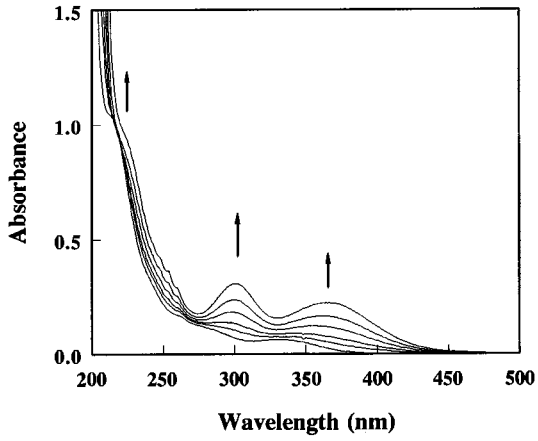

Fig. 2. Spectral changes resulting from the photolysis of $Ru(\eta^6\text{-bz})_2^{2+}$ in CH_3CN. Spectra were acquired after 0, 1.0, 2.2, 3.5, 4.6 and 6.0 min of irradiation at 365 nm; arrows indicate the direction of the absorbance changes. Similar changes occur upon photolysis at 254 nm, at 313 nm, and with Pyrex-filtered (>290 nm) light.

some degree of arene-to-metal charge transfer (mesitylene has a lower first ionization energy than benzene [11]) and/or intraligand $\pi-\pi^*$ character (the singlet $\pi-\pi^*$ transitions of mesitylene lie at lower energies than those of benzene [11]).

Ultraviolet irradiation of $Ru(\eta^6\text{-bz})_2^{2+}$ in non-deaerated CH_3CN causes the spectral changes depicted in Fig. 2. Two prominent bands appear in the region above 290 nm, while fine structure attributable to free benzene (Fig. 1) becomes evident around 250 nm. Further characterization of the photoreaction was facilitated by ^{1}H-NMR spectroscopy. In CD_3CN solution the parent complex exhibits a singlet at 6.82 ppm arising from the protons of the coordinated rings. Photolysis causes the appearance of additional singlets at 7.39 and 6.19 ppm, which are assignable to the protons of free benzene and $Ru(\eta^6\text{-bz})(CD_3CN)_3^{2+}$, respectively, by comparison to the spectra of authentic samples. The signal areas of these two photoproducts are equal to at least 25% conversion, indicating that $Ru(\eta^6\text{-bz})_2^{2+}$, like $Ru(\eta^6\text{-mes})_2^{2+}$, undergoes clean photosubstitution of one arene ligand by solvent (Eq. 1).

Table 1 lists arene substitution quantum yields (Φ_{arene}) determined for $Ru(\eta^6\text{-bz})_2^{2+}$ in the present study and, for comparison, the corresponding data obtained previously for $Ru(\eta^6\text{-mes})_2^{2+}$ [2]. Since both complexes are thermally robust ($<1\%$ reaction after 1 week) on the time scale of the photochemical experiments, dark corrections to Φ_{arene} were unnecessary. Neither complex exhibits a significant dependence of Φ_{arene} upon the excitation wavelength, suggesting that the high-lying electronic states populated via light absorption undergo efficient relaxation to a common, lower-energy excited state from which reaction occurs. We investigated the nature of this photoactive state in a series of sensitization experiments that employed the triplet sensitizer, acetophenone. This organic carbonyl compound undergoes intersystem crossing from its excited singlet manifold to the lowest triplet state with unit efficiency [12]; moreover, the available triplet energy (ca. 74 kcal [13]) is sufficient to populate the lowest ligand field triplet state of $Ru(\eta^6\text{-mes})_2^{2+}$ (<70 kcal) via classical electronic energy transfer. We find that photoexcitation of acetophenone in deoxygenated CH_3CN solutions containing the Ru(II) complex results in sensitized substitution of one mesitylene ligand by solvent (Eq. 1). Most importantly, the limiting value of Φ_{arene} determined in these sensitization experiments, 0.15 ± 0.02, closely matches Φ_{arene} measured in direct photolysis (Table 1). This finding provides experimental support for the proposal that arene substitution originates entirely from the lowest ligand field triplet of $Ru(\eta^6\text{-arene})_2^{2+}$ complexes [1]. This state arises from the one-electron transition between a molecular orbital that is essentially d_z^2 in character and nonbonding, and a higher-energy, predominantly metal-centered molecular orbital that is antibonding with respect to the metal–ligand bonds [1,14]. The redistribution of electron density that results from this transition weakens the Ru–arene bonding and creates an energetically low-lying vacancy in the d_z^2 orbital that facilitates attack on the metal center by solvent. The photoactive triplet state must be quite short lived, since our earlier study [2] revealed that O_2 does not quench arene photosubstitution. Assuming a diffusion-controlled quenching rate, we estimate a triplet lifetime of <10 ns.

The marked drop in Φ_{arene} that accompanies the introduction of methyl substituents to the arene ring (Table 1) finds precedence in the studies of Mann et al. [15,16] and Karlen et al. [1], who noted that both steric and electronic effects may contribute to this behavior. Sterically, the larger size of CH_3 relative to H more effectively shields the metal from nucleophilic attack by solvent and, in so doing, hinders the formation of the

Table 1
Photosubstution quantum yields for $Ru(\eta^6\text{-arene})_2^{2+}$ complexes in CH_3CN

Wavelength (nm)	$Ru(\eta^6\text{-mes})_2^{2+}$	$Ru(\eta^6\text{-bz})_2^{2+}$
	Φ_{arene}^a	
254	0.15 ± 0.00 (3)	0.56 ± 0.02 (3)
313	0.16 ± 0.00 (3)	0.55 ± 0.02 (3)
365	0.11 ± 0.01 (4)	0.48 ± 0.01 (3)

[a] Quantum yield for substitution of one arene ligand by solvent. Error limits represent average deviation from the mean for two or more runs; number of runs indicated in parentheses. The estimated accuracy of the quantum yields is ± 10–15%.

Table 2
Electronic absorption spectral data for Ru(η^6-arene)$(L)_3^{2+}$ complexes inCH_3CN solution

Complex	Band position (nm)	ε (M^{-1} cm^{-1})
Ru(η^6-mes)$(CH_3CN)_3^{2+}$	234 (sh)	923
	254 (sh)	539
	304	775
	369	638
	230	1377
Ru(η^6-bz)$(CH_3CN)_3^{2+}$	253 (sh)	623
	302	796
	365	624
	233	694
Ru(η^6-mes)$(NH_3)_3^{2+}$	258	637
	297	607
	362	490
	226	1335
Ru(η^6-bz)$(NH_3)_3^{2+}$	258	796
	295	695
	358	471

ring-slipped intermediate, **I**. Electronically, the electron-donating inductive effect of CH_3 strengthens metal–ring bonding and thereby increases the likelihood that the ring-slipped arene in **I** will displace coordinated solvent to regenerate the parent complex. While the previous workers reached different conclusions regarding the relative importance of these effects in determining the photoreactivity of Ru(II) sandwich complexes containing highly methylated rings, there was general agreement that the inductive effect dominates in cases, such as Ru(η^6-bz)$_2^{2+}$ and Ru(η^6-mes)$_2^{2+}$, where the arene ring bears three or fewer CH_3 groups.

3.2. Spectroscopy and photochemistry of Ru(η^6-arene)L_3^{2+} complexes

Table 2 summarizes electronic spectral data for the Ru(η^6-arene)$(L)_3^{2+}$ complexes (L is CH_3CN or NH_3) examined in this study. Each complex displays four absorption features between 225–370 nm which, by analogy to the earlier work of Weber and Ford [3], are assigned as spin-allowed ligand field transitions. The changes in electron density associated with these transitions can be described in terms of the qualitative molecular orbital scheme depicted in Fig. 3 [3]. The lowest-energy ligand field transition, $^1A_1 \rightarrow {}^1E$, corresponds to the excitation of one electron from the filled a_1 orbital to the empty 3e* orbitals. The a_1 orbital is essentially nonbonding with respect to the Ru–L bonds and moderately π-antibonding toward the Ru–arene bonds, while the degenerate 3e* orbitals are σ-antibonding with respect to both types of metal–ligand bonds [17]. The three higher-lying transitions, $^1A_1 \rightarrow {}^1E$, ^1A_l, $^1A_2$, correlate with the 2e to 3e* one-electron

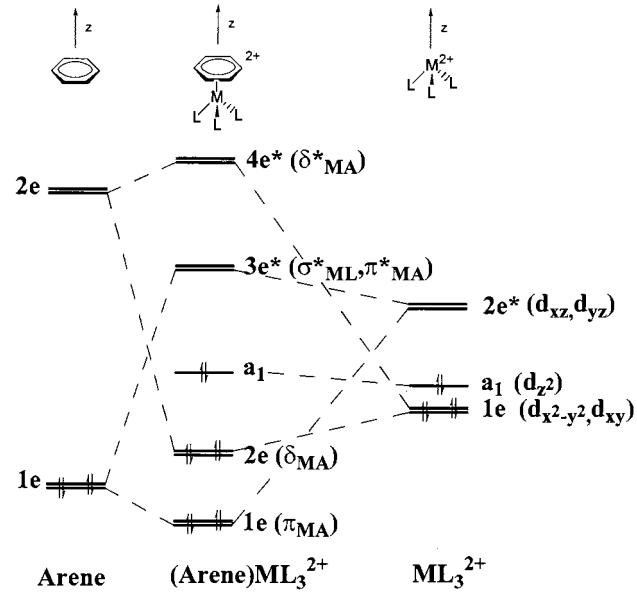

Fig. 3. Qualitative molecular orbital diagram for a Ru(η^6-arene)$(L)_3^{2+}$ complex; C_{3v} geometry assumed (after Fig. 3 in [3]). MA and ML refer to metal-arene and metal-NH_3 or M-$NCCH_3$ bonds, respectively, while the asterisk denotes antibonding character.

excitation. The Ru–arene interaction in the 2e molecular orbitals is weakly bonding owing to poor (δ-type) overlap, while the Ru–L interaction is approximately nonbonding for the σ-donor ligand, NH_3, and π-bonding for the π-donor ligand, CH_3CN.

Table 3
Photosubstitution quantum yields for Ru(η^6-mes)$(L)_3^{2+}$ complexes in CH_3CN

Complex	Φ^a_{arene}	Φ^a_L
	254 nm	
Ru(η^6-mes)$(CH_3CN)_3^{2+}$	0.0024 ± 0.0002 (2)	0.47 ± 0.10 (3)
Ru(η^6-bz)$(CH_3CN)_3^{2+}$	0.013 ± 0.000 (3)	0.60 ± 0.16 (6)
Ru(η^6-mes)$(NH_3)_3^{2+}$	0.0255 (1)	0.065 (1)
Ru(η^6-bz)$(NH_3)_3^{2+}$	0.043 (1)	0.073 (1)
	313 nm	
Ru(η^6-mes)$(CH_3CN)_3^{2+}$	0.0011 ± 0.0003 (3)	0.42 ± 0.08 (3)
Ru(η^6-bz)$(CH_3CN)_3^{2+}$	0.0066 ± 0.0001 (2)	Not determined
Ru(η^6-mes)$(NH_3)_3^{2+}$	<0.002	0.047 ± 0.005 (2)
Ru(η^6-bz)$(NH_3)_3^{2+}$	0.041 ± 0.011 (4)	0.043 ± 0.010 (4)
	365 nm	
Ru(η^6-mes)$(CH_3CN)_3^{2+}$	0.00028 ± 0.00004 (2)	0.18 ± 0.01 (2)
Ru(η^6-bz)$(CH_3CN)_3^{2+}$	0.0020 ± 0.0001 (2)	0.40 ± 0.10 (6)
Ru(η^6-mes)$(NH_3)_3^{2+}$	<0.0008	0.029 (1)
Ru(η^6-bz)$(NH_3)_3^{2+}$	0.0099 (1)	0.013 (1)

[a] Quantum yield for substitution of one arene ligand (Φ_{arene}) or one monodentate ligand (Φ_L) by solvent. Error limits represent average deviation from the mean for two or more runs; number of runs indicated in parentheses. The estimated accuracy of the quantum yields is $\pm$ 20–30%.

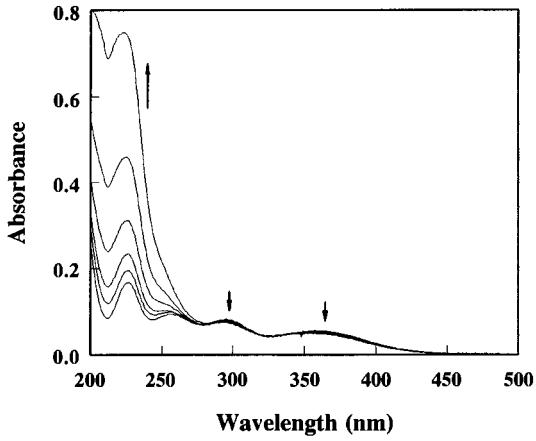

Fig. 4. Spectral changes arising from the photolysis of Ru(η^6-bz)$(NH_3)_3^{2+}$ in CH_3CN. Spectra were measured in a 1.0 mm pathlength cell after irradiating the sample for 0, 100, 300, 600, 1100, and 2100 s at 365 nm in a 1.0 cm pathlength cell; arrows indicate the direction of the absorbance changes.

The thermal and photochemical reactions of Ru(η^6-bz)$(CH_3CN)_3^{2+}$ in CD_3CN closely parallel those observed for Ru(η^6-mes)$(CH_3CN)_3^{2+}$ (Eq. 2a, b). Thermal exchange of coordinated CH_3CN with solvent occurs for both complexes with a pseudo first-order rate constant of $3.60 \pm 0.07 \times 10^{-5}\ s^{-1}$ at 20 ± 1°C. Ultraviolet irradiation accelerates this exchange and also induces arene deligation. Table 3 lists the quantum yields, Φ_L and Φ_{arene}, for these photosubstitution processes as a function of excitation wavelength.

In contrast to the thermal lability of the monodentate ligands in Ru(η^6-arene)$(CH_3CN)_3^{2+}$, no detectable substitution of NH_3 by solvent occurs for Ru(η^6-bz)$(NH_3)_3^{2+}$ in CD_3CN after one week at room temperature. This robustness of coordinated NH_3 is consonant with previous work [3] that found no NH_3 loss from several Ru(η^6-arene)$(NH_3)_3^{2+}$ complexes in acidified water over several weeks. As seen in Fig. 4, ultraviolet irradiation of Ru(η^6-bz)$(NH_3)_3^{2+}$ in CH_3CN results in a large increase in the short-wavelength region of the electronic spectrum, accompanied by a much smaller bleaching of the long-wavelength bands. Detailed identification of the photoproducts was accomplished by ^{1}H-NMR spectroscopy. The spectrum of Ru(η^6-bz)$(^{15}NH_3)_3^{2+}$ exhibits a singlet at 5.77 ppm attributable to coordinated benzene and a doublet ($^1J_{NH} = 71$ Hz) centered at 2.89 ppm arising from the ammine ligands. Ultraviolet irradiation causes the appearance of an arene singlet at 5.89 ppm, a singlet at 7.39 ppm due to free benzene, a doublet centered at 3.03 ppm, and additional doublets in the region from 1.9 to 2.5 ppm. All doublets possess a coupling constant of 71 Hz, indicating that they arise from protons bound to ^{15}N. The signals at 3.03 and 5.89 ppm are assigned to the ammine and benzene protons, respectively, of Ru(η^6-bz)$(^{15}NH_3)_2(CD_3CN)^{2+}$, in agreement with the 1:1 ratio of signal areas that persists throughout the course of photolysis. The doublets appearing between 1.9 and 2.5 ppm are attributable to free $^{15}NH_3$ and $Ru(^{15}NH_3)_3(CD_3CN)_3^{2+}$ (note that *fac* and *mer* isomers are possible). Collectively, these results establish that Ru(η^6-bz)$(NH_3)_3^{2+}$ undergoes competitive photosubstitution of arene (Eq. 3a) and ammine (Eq. 3b) ligands by solvent. Electronic and ^{1}H-NMR spectral changes similar to those just described occur upon photolysis of Ru(η^6-mes)$(NH_3)_3^{2+}$ in CH_3CN, indicating that this complex also undergoes arene and ammine photosubstitution. Quantum yield data for both triammine complexes are compiled in Table 3.

$$Ru(\eta^6\text{-bz})(NH_3)_3^{2+} \xrightarrow{h\nu} \begin{cases} \xrightarrow{CH_3CN} Ru(NH_3)_3(CH_3CN)_3^{2+} + bz & (3a) \\ \xrightarrow{CH_3CN} Ru(\eta^6\text{-bz})(NH_3)_2(CH_3CN)^{2+} + NH_3 & (3b) \end{cases}$$

Fig. 5 provides a mechanistic framework for discussing the photochemical behavior of the Ru(η^6-arene)$(L)_3^{2+}$ family. Photoexcitation of a complex (denoted by an asterisk) at wavelengths ≥ 254 nm populates ligand field excited states that can interact with solvent via two pathways. In path A, the substitution of a labilized monodentate ligand by solvent yields Ru(η^6-arene)$(L)_2S^{2+}$. Alternatively, the cleavage of one metal–arene bond in path B generates an intermediate, **II**, containing an η^4-bonded arene ring and a coordinated solvent molecule. This ring-slipped intermediate then partitions among several pathways that lead to stable products. Sequential breaking of the remaining metal–ring bonds in path C results in complete substitution of the arene by solvent to produce $Ru(L)_3(S)_3^{2+}$. Competing with this process is recoordination of the third metal–arene bond via displacement of a monodentate ligand. Loss of the solvent molecule in path D regenerates the parent complex, while loss of an L ligand in path E yields Ru(η^6-arene)$(L)_2S^{2+}$.

Certain features of this mechanism should be noted. First, the formation of the monosubstituted product, Ru(η^6-arene)$(L)_2S^{2+}$, occurs via both direct (path A) and indirect (path B followed by path E) routes. Second, while Ru(η^6-arene)$(L)_3^{2+}$ complexes undergo photosubstitution of arene much less efficiently (Table 3) than the corresponding Ru(η^6-arene)$_2^{2+}$ complexes (Table 1), Φ_{arene} for both families drops upon switching the arene from benzene to mesitylene. This parallel response to increasing ring methylation suggests some

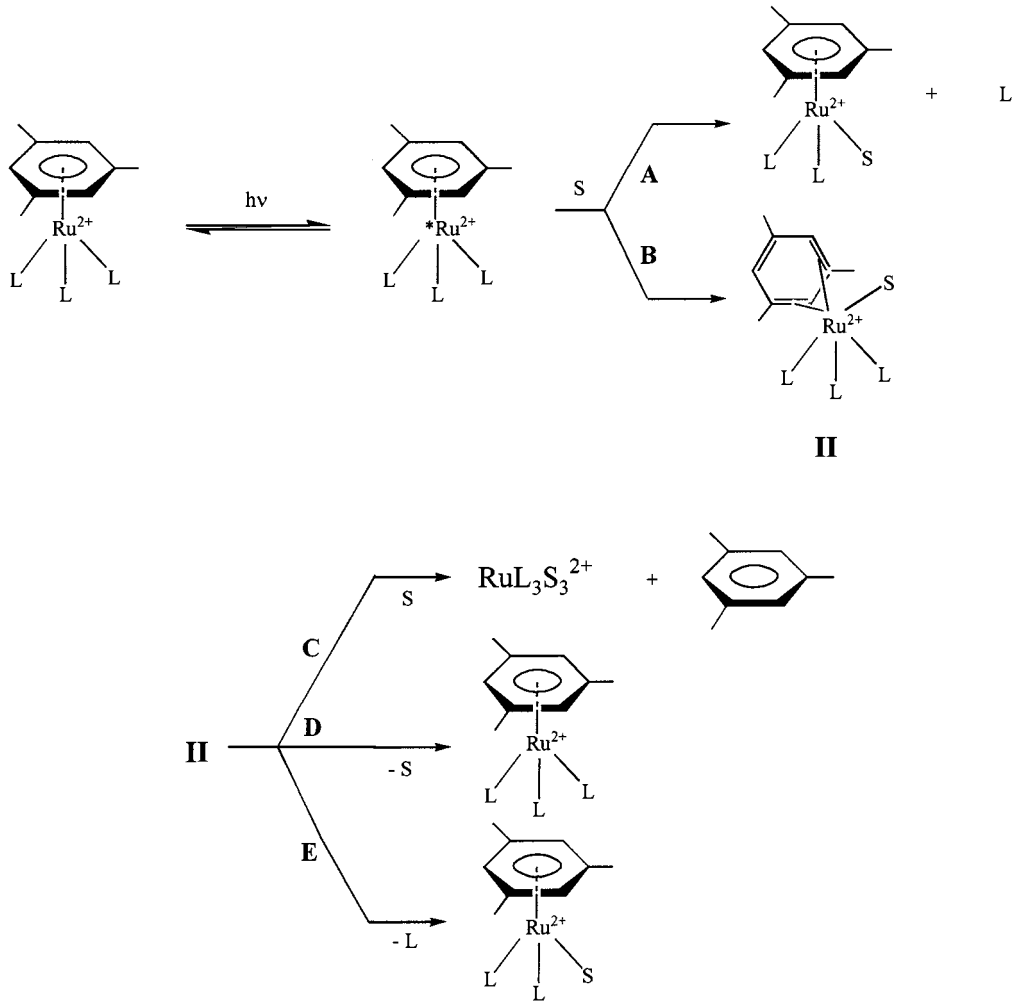

Fig. 5. Mechanistic scheme for the photosubstitution reactions of Ru(η^6-arene)$(L)_3^{2+}$ complexes in CH_3CN.

commonality of mechanism. One obvious similarity is the involvement of the ring-slipped intermediates, **I** and **II**, whose proclivities toward recoordination of the third metal–arene bond, and thus toward smaller Φ_L values, should increase as more electron-donating CH_3 groups reside on the rings. Lastly, in contrast to the behavior of Ru(η^6-arene)$_2^{2+}$ complexes, members of the Ru(η^6-arene)$(L)_3^{2+}$ family undergo photosubstitution with wavelength-dependent quantum yields. Moreover, as seen in Table 4, the Φ_L/Φ_{arene} ratio increases at longer excitation wavelengths for Ru(η^6-mes)$(CH_3CN)_3^{2+}$, Ru(η^6-bz)$(CH_3CN)_3^{2+}$, and Ru(η^6-mes)$(NH_3)_3^{2+}$. The variability of this ratio requires the involvement of at least two reactive excited states in the photosubstitutional chemistry of these half-sandwich complexes. On the basis of the present data, we cannot distinguish between the case in which arene loss originates from one state and ammine loss from another state, and the case in which two (or more) states undergo both reactions albeit with different Φ_L/Φ_{arene} ratios. Nonetheless, it is clear from the wavelength response of the ratio that arene release becomes relatively more important at higher excitation energies. The wavelength insensitivity

Table 4
Ratios of the photosubstitution quantum yields for Ru(η^6-arene)$(L)_3^{2+}$ complexes in CH_3CN

Complex	254 nm	313 nm	365 nm
	Φ_L/Φ_{arene}		
Ru(η^6-mes)$(CH_3CN)_3^{2+}$	200 ± 60[a]	380 ± 180[a]	710 ± 55[a]
Ru(η^6-bz)$(CH_3CN)_3^{2+}$	46 ± 12[a]	Not determined	200 ± 60[a]
Ru(η^6-mes)$(NH_3)_3^{2+}$	2.6 ± 0.7[b]	>23.5	>36.3
Ru(η^6-bz)$(NH_3)_3^{2+}$	1.7 ± 0.5[b]	1.0 ± 0.6[a]	1.3 ± 0.3[b]

[a] Error limits calculated by propagating the errors (average deviation from the mean) for each quantum yield.
[b] For those quantum yields without an average deviation from the mean, the standard deviation of the quantum yield, determined from the linear least-squares fit, was used to calculate the error limits in the quantum yield ratios.

of Φ_L/Φ_{arene} for $Ru(\eta^6\text{-bz})(NH_3)_3^{2+}$ is surprising, given the similarity of its absorption spectrum to that of $Ru(\eta^6\text{-mes})(NH_3)_3^{2+}$ (Table 2). While such behavior is consistent with arene and ammine loss originating from a single excited state, an equally plausible explanation is that two excited states undergo both reactions with comparable Φ_L/Φ_{arene} ratios.

We noted in the Introduction that our previous study [2] of $Ru(\eta^6\text{-mes})(CH_3CN)_3^{2+}$ in CH_3CN revealed efficient photosubstitution of coordinated CH_3CN by solvent, whereas Weber and Ford [3] found negligible photolabilization of NH_3 from $Ru(\eta^6\text{-bz})(NH_3)_3^{2+}$ in aqueous solution. Data collected in Table 3 can be used to assess the importance of factors (i–iii) that were cited as possible causes of this disparity. Changing the arene from benzene to mesitylene (factor (i)) has relatively little effect as seen from a comparison of Φ_L values for corresponding $Ru(\eta^6\text{-bz})(L)_3^{2+}$ and $Ru(\eta^6\text{-mes})(L)_3^{2+}$ complexes. The nature of the solvent medium (factor (iii)), on the other hand, appears to play a more important role. Thus, Weber and Ford reported quantum yields for ammine loss from $Ru(\eta^6\text{-bz})(NH_3)_3^{2+}$ in aqueous solution that, depending upon the excitation wavelength, are at least 25–150 times smaller than those measured by us for this complex in CH_3CN. Interestingly, the quantum yields for arene loss from the complex are quite similar in the two studies, implying that solvent selectively affects one of the two photosubstitution pathways.

Changing the monodentate ligand (factor (ii)) can influence Φ_L in ways that are best discussed by reference to the mechanism presented in Fig. 5. In the pathway involving direct substitution of L by solvent (path A), the extent of Ru–L bond labilization in an excited state should be an important determinant of photoreactivity. Exciting the $2e \rightarrow 3e^*$ one-electron transition (Fig. 3) depopulates a molecular orbital that is π-bonding between Ru and CH_3CN but essentially nonbonding between Ru and NH_3, while it populates an orbital that is σ-antibonding with respect to both types of metal–ligand bonds. These changes in electron density might be expected to cause greater labilization of the $Ru-NCCH_3$ bonds, thus accounting for the larger Φ_L values obtained at shorter excitation wavelengths for complexes containing CH_3CN (Table 3). Similar reasoning does not explain the preferential loss of this ligand upon exciting the lower-energy $a_1 \rightarrow 3e^*$ transition, since the a_1 molecular orbital is largely nonbonding with respect to the $Ru-NH_3$ and $Ru-NCCH_3$ bonds. In this case, a possible explanation takes account of the substitutional labilitity of L in intermediate **II**. Recall that, in $Ru(\eta^6\text{-arene})(L)_3^{2+}$ complexes, CH_3CN undergoes thermal substitution by solvent much more rapidly than NH_3. Accordingly, we might expect that displacement of L via recoordination of the third metal–arene bond (path E) would be more facile, and thereby yield higher Φ_L values, when $L = CH_3CN$.

Acknowledgements

We thank Professor A. Ludi for providing some spectral information about $Ru(\eta^6\text{-arene})_2^{2+}$ complexes. Financial support for this work was received from the National Science Foundation (Grant DMR-9122653).

References

[1] T. Karlen, A. Hauser, A. Ludi, Inorg. Chem. 33 (1994) 2213–2218.
[2] R.J. Lavallee, C. Kutal, J. Photochem. Photobiol. A: Chem. 103 (1997) 213–220.
[3] W. Weber, P.C. Ford, Inorg. Chem. 25 (1986) 1088–1092.
[4] T. Karlen, A. Ludi, A. Muhlebach, P. Bernhard, C. Pharisa, J. Polym. Sci. Part A 33 (1995) 213–220.
[5] G. Gamble, C. Kutal, Polym. Adv. Technol. 5 (1994) 63–69.
[6] M.A. Bennett, A.K. Smith, J. Chem. Soc. Dalton Trans. (1974) 233–241.
[7] M.I. Rybinskaya, A.R. Kudinov, V.S. Kaganovich, J. Organomet. Chem. 246 (1983) 279–285.
[8] C.G. Hatchard, C.A. Parker, Proc. R. Soc. London Ser. A 235 (1956) 518–536.
[9] W.H. Morrison Jr., E.Y. Ho, D.A. Hendrickson, Inorg. Chem. 14 (1975) 500–506.
[10] V. Balzani, F. Bolletta, F. Scandola, J. Am. Chem. Soc. 102 (1980) 2152–2163.
[11] H.H. Jaffe, M. Orchin, Theory and Applications of Ultraviolet Spectroscopy, John Wiley, New York, 1962, Ch. 12.
[12] S.K. Chattopadhyay, C.V. Kumar, P.K. Das, J. Photochem. 30 (1985) 81–91.
[13] S.L. Murov, I. Carmichael, G.L. Hug, Handbook of Photochemistry, 2nd ed., Marcel Dekker, New York, 1993, p. 91.
[14] D.W. Clack, K.D. Warren, Inorg. Chim. Acta 30 (1978) 251–258.
[15] A.M. McNair, J.L. Schrenk, K.R. Mann, Inorg. Chem. 23 (1984) 2633–2640.
[16] J.L. Schrenk, A.M. McNair, F.B. McCormick, K.R. Mann, Inorg. Chem. 25 (1986) 3501–3504.
[17] T.A. Albright, J.K. Burdett, M. Whangbo, Orbital Interactions in Chemistry, John Wiley, New York, 1985, Ch. 20.